

EXPLORING DISCONTINUITIES AND HYBRIDIZATION TO DESIGN GRADUAL FAILURE IN UNIDIRECTIONAL CARBON FIBER/SELF-REINFORCED POLYPROPYLENE COMPOSITES

Jun Tang¹, Arya Aslani¹, Yentl Swolfs¹, Gianmaria Bullegas²,
Silvestre T. Pinho², Stepan V. Lomov¹, Larissa Gorbatikh¹

¹Department of Materials Engineering, KU Leuven, Kasteelpark Arenberg 44 bus 2450,
3001 Leuven, Belgium

²Department of Aeronautics, Imperial College London, South Kensington Campus,
SW7 2AZ London, United Kingdom

Email: jun.tang@kuleuven.be, web page: www.composites-kuleuven.be

Keywords: Discontinuities, Tensile behavior, Failure mechanisms, Hybrid composites

ABSTRACT

Both discontinuous fiber-reinforced composites and hybrid composites show the potential to overcome the stiffness-toughness dilemma that conventional fiber reinforced polymer composites suffer from. To fully utilize the advantages of discontinuities and hybridization, careful design of the configuration of discontinuities is required. In this paper, high-precision fiber cuts with a staggered pattern were introduced in the unidirectional carbon fiber layer of hybrid carbon fiber/self-reinforced polypropylene composites. This aimed to control the failure mechanisms, hence targeting a gradual failure in tension. The effect of the geometrical parameters of the patterns, including cut length, cut fraction and step length, were investigated. The tensile behavior of the hybrids was influenced by a combined effect of these three parameters. The hybrids exhibited three types of the failure behavior: 1) single fracture of the carbon fiber layer followed by single delamination growth, 2) carbon fiber layer fragmentation accompanied by multiple delamination growth and 3) multiple delamination growth without carbon fiber layer fracture. In the regime of carbon fiber layer fragmentation accompanied by multiple delamination growth, a gradual failure with relatively high damage resistance was achieved.

1 INTRODUCTION

Strong evidence exists that the unique mechanical properties (particularly toughness) of biological materials stem from their intelligent structural organization. Naturally occurring composites such as nacre, bone and silk are made of discontinuous reinforcements assembled in a hierarchical fashion [1, 2]. These biological materials have been shown to escape from the stiffness-toughness dilemma of conventional fiber reinforced composites and therefore serve as an inspiration for design of tough engineering materials. Composites based on discontinuous random fibers, or fiber strands, are attracting interest of the automobile industry due to their low cost and excellent formability [3, 4]. However, their stiffness and strength are much lower than those of continuous fiber composites. This is due to the intrinsic heterogeneity of their microstructure, random orientation of fibers and stress concentrations at the fiber/strand ends. To improve the strength and stiffness of the discontinuous fiber reinforced composites, one would need to align fibers unidirectionally [5-7] and to optimize their length [8]. The toughness, on the other hand, can be increased by carefully designing the discontinuity configuration [9, 10].

The other promising way of overcoming the stiffness-toughness dilemma is hybridization of different fiber types. Hybridizing stiff but brittle fibers with ductile but compliant fibers in unidirectional composites has shown to yield hybrid composites with relatively high stiffness as well as high ductility compared to the non-hybrid materials [11-13]. Despite this success, the gradual failure development up to high strains has been elusive. The main challenge in this type of hybrid composites has been to avoid the significant stress drop when brittle component fails. This means hybridization alone seems to have limitations for certain combinations of fibers, for example carbon fibers and polypropylene (PP) tapes.

Interestingly, the research on combining discontinuities and hybridization is quite limited. Preliminary research [14] indicates that a partially cut carbon fiber ply at critical locations influences the tensile behavior of the hybrid carbon fiber/self-reinforced polypropylene (SRPP) composites. Larger cuts were found to trigger carbon fiber layer fragmentation, which lowered the stress upon carbon fiber layer fracture while maintaining most of the ductility, hence resulting in a relatively gradual failure compared to hybrid carbon fiber/SRPP composites without any cuts. Similarly, in the work of Czél et al. [15], where the entire width of the carbon fiber layer was cut, the discontinuities led to the layer fragmentation and a gradual failure, termed as pseudo-ductile behavior.

The aim of this work is to further explore the potential of discontinuities focusing on more complex meso-level patterns. The design of the patterns is based on the work of Bullegas et al.[8], where staggered laser cuts were introduced to successfully deflect the crack propagation. The creation of fiber bundle pull-out allowed to dissipate more energy and thus significantly increased the toughness. We investigate the effect of discontinuities on the specific case of hybrid carbon fiber/SRPP composites, but the proposed concepts are universal and can be applied to other hybrid composites.

2 MATERIALS AND METHODS

2.1 Materials

Three raw materials were used in this study: carbon fiber preform, PP film and woven PP tape fabric. Carbon fiber preforms with an areal density of 73 g/m² were provided by Chomarac (France). The fiber type was T700SC-50C and all the fibers were unidirectionally aligned without binder. Propex Fabrics GmbH (Germany) supplied the PP film as well as the woven PP tape fabric and both of them were composed of the same PP grade. The PP film was 20 µm thick and had a density of 0.92 g/cm³. The woven PP tape fabric had a twill 2/2 weave pattern and the areal density of 130 g/m². The weave was overfed, thus the spacing between two adjacent PP tapes was smaller than the nominal tape width. Therefore, some of the PP tapes were folded [16].

2.2 Manufacturing

The manufacturing of hybrid carbon fiber/SRPP composites with staggered discontinuities followed three steps: 1) carbon fiber prepreg production, 2) laser micro-milling of discontinuities, and 3) hybrid composites production.

A single layer of the unidirectional carbon fiber preform as well as two PP films were cut into 290×150 mm dimensions and put into a copper mold with one PP film above the carbon preform and the other one below. The mold was inserted into a hot press, which was preheated at 188°C. The stack was hot pressed at 188°C for 5 minutes at a pressure of 5 bar to impregnate carbon fibers.

After carbon fiber prepreps had been made, laser micro-milling was used to introduce cuts in the prepreps with designed patterns. All the cuts were perpendicular to the fiber direction, see Fig.1. The diameter of the laser beam of the laser machine (Oxford Lasers, Series A) ranged from 10 to 15 µm. This vaporized the material locally and ensured a precise cut [10].

The layup of hybrid carbon fiber/SRPP composites was S₃/F/C/F/S₃, where S stands for SRPP, F for PP film and C for the carbon fiber prepreg with laser cuts. Two additional interleaved PP films were used to create more matrix, hence improving bonding between the carbon fiber prepreg and the neighboring SRPP layers. The layup was hot compacted at 188°C, 39 bar for 5 minutes and cooled down to 40°C in 5 minutes while maintaining the high pressure. Compared to 5 bar for carbon fiber impregnation, 39 bar was used in this case to prevent shrinkage of PP tapes.

The schematics of the front and through-thickness views of the specimen are shown in Fig. 1 and all the cutting pattern parameters are listed in Table 1. As illustrated in Fig.1, the staggered cutting pattern

was repeated three times along the specimen length with a distance of 40 mm in-between, which aimed to trigger carbon fiber layer fracture at these three locations. Fourteen staggered cutting patterns were designed to investigate the effect of cut fraction (F , the fraction of cut fibers within one staggered pattern), cut length (C , the length of a single laser cut) and step length (S , the longitudinal distance between two laser cuts within one staggered pattern).

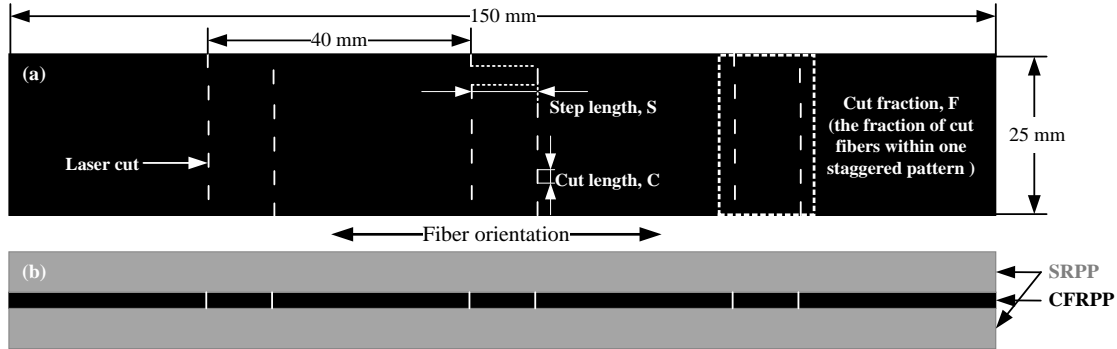


Figure 1: Schematic of a hybrid carbon fiber/SRPP composite specimen with staggered laser cuts in the carbon fiber layer: (a) front view of the hybrid composites with annotations on cut fraction, cut length and step length, (b) through-thickness view of the hybrid composites

Pattern number	1	2	3	4	5	6	7	8	9	10	11	12	13	14
Cut fraction, F	0.4	0.4	0.4	0.4	0.6	0.6	0.6	0.6	1	1	1	1	1	1
Cut length, C (mm)	0.25	0.25	1	1	0.25	0.25	1	1	0.25	0.25	0.25	1	1	1
Step length, S (mm)	2	5	2	5	2	5	2	5	2	5	10	2	5	10

Table 1: Cutting pattern parameters

2.3 Tensile test

Tensile tests were performed according to ASTM D3039 at a displacement rate of 0.125 mm/s. The nominal dimensions of the sample were 250 mm×25 mm×1 mm, with a gauge length of 150 mm. The tests were monitored by two digital cameras imaging the front and back sample surfaces during the test. These images were processed with digital image correlation to measure strains and were used to analyze the failure mechanisms. Five samples of each configuration were tested.

2.4 Failure mechanisms

Two main failure mechanisms are discussed in this study: carbon fiber layer fracture, and delamination of layers. The delamination could be observed due to the translucency of SRPP. Whitening appearing on the sample surface image indicated the initiation of delamination, while enlarging of the white region revealed the propagation of delamination.

Regarding the carbon fiber layer fracture, when the cut fraction (F) was lower than 1, the carbon fiber layer fractured at a certain strain caused by the breakage of remaining continuous fibers. This could be easily observed from the triggering of delamination. However, once all the fibers were cut ($F=1$), it was not straightforward to detect the carbon fiber layer fracture, because the delamination could also be triggered by fiber bundle pull-out. Therefore, post-mortem fracture surface was observed to determine whether the carbon fiber layer was fractured. Possible failure mechanisms in the carbon fiber layer are shown in Fig.2. The number of fractures was also counted to analyze how the discontinuities affected the fracture behavior of carbon fiber layer in the hybrids.

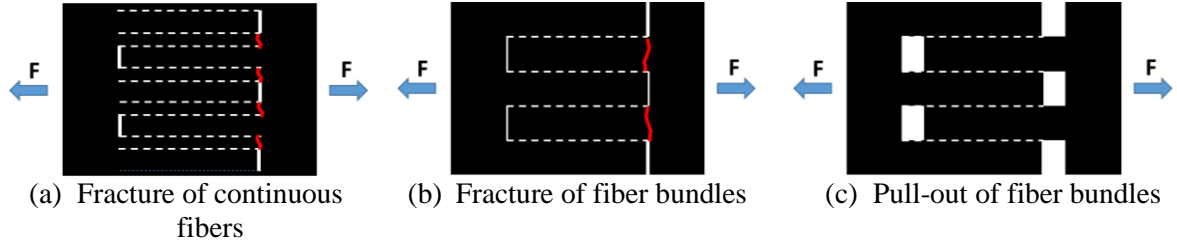


Figure 2: Schematics of fracture behavior in the carbon fiber layer

3 RESULTS

The results are split into three parts to understand how the cut fraction, cut length and step length influence the tensile behavior. Following this, a more concise analysis is carried out.

To facilitate the following discussion, the average number of ply fractures, represented by N , for each pattern is listed in Table 2. This value is calculated by counting the number of ply fractures for every sample of each pattern, hence, it reveals the probability of having more fractures to some extent. When the cut fraction is lower than 1 (pattern 1 to pattern 8), all the ply fractures are attributed to the fracture of continuous fibers, see Figure 2(a). When the cut fraction is equal to 1, the carbon fiber ply failure is either caused by the fracture of fiber bundles ($N > 1$), see Figure 2(b), or caused by the pull-out of fiber bundles ($N = 0$), see Figure 2(c).

Pattern number as in Table 1	Cutting pattern name	Average number of carbon ply fractures, N
1	F0.4-C0.25-S2	1
2	F0.4-C0.25-S5	1
3	F0.4-C1-S2	1
4	F0.4-C1-S5	1
5	F0.6-C0.25-S2	2.6
6	F0.6-C0.25-S5	1
7	F0.6-C1-S2	2
8	F0.6-C1-S5	1.75
9	F1-C0.25-S2	0
10	F1-C0.25-S5	2.6
11	F1-C0.25-S10	1.4
12	F1-C1-S2	0
13	F1-C1-S5	0
14	F1-C1-S10	3

Table 2: Average number of fractures for every cutting pattern

3.1 Effect of the cut fraction

Figure 3 shows the stress-strain diagrams of the hybrid composites with a fixed cut length of 0.25 mm and a fixed step length of 2 mm, but with an increasing cut fraction. Compared to the reference hybrids without cuts, the presence of laser cuts significantly reduced the peak stress upon carbon fiber layer fracture. This is caused by the stress concentrations around the laser cut, which leads to carbon fiber layer failing earlier than the carbon fiber failure strain (2%). With larger cut fractions, less continuous fibers remained, hence less energy was released when the carbon fiber layer fractured, which resulted in the decrease of the stress drop. When all the fibers were cut ($F=1$), the delamination was induced by fiber bundle pull-out instead of carbon fiber breakage, hence no stress drop was observed. In this case, the stress strain curve starts deviating from the linear region at a very low overall strain, which indicates a low damage resistance.

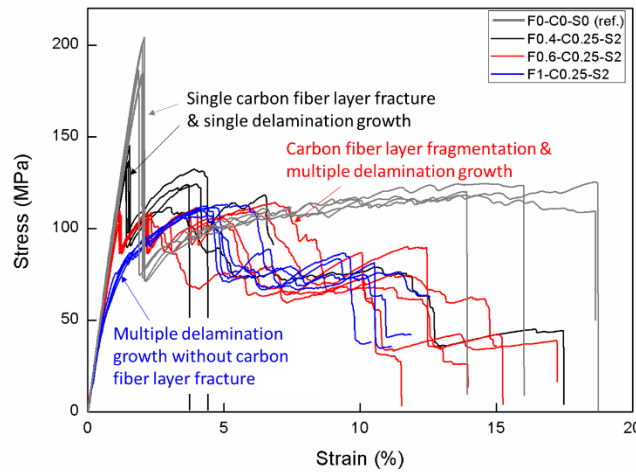


Figure 3: Stress-strain diagrams of pattern 1 (F0.4-C0.25-S2), pattern 5 (F0.6-C0.25-S2), Pattern 9 (F1-C0.25-S2) and reference hybrids without cuts

Similar changes were found for other cut and step lengths as illustrated in Figure 4 and Figure 5. This leads to the conclusion that, with a fixed cut length and step length, the tensile behavior was significantly altered by increasing the cut fraction. More carbon fiber layer fractures were triggered when the cut fraction increased to 0.6, but fully cutting fibers led to fiber bundle pull-out rather than to carbon fiber fracture.

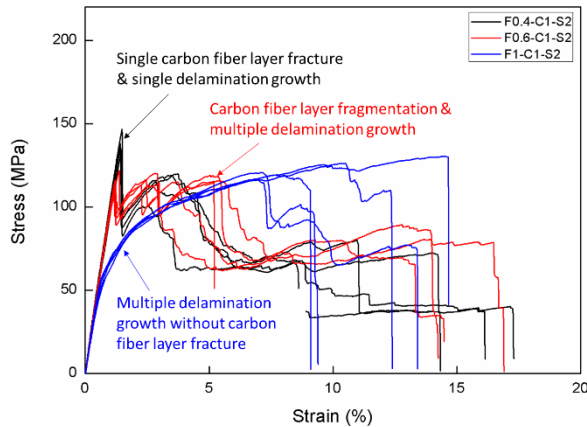


Figure 4: Stress-strain diagrams of pattern 3 (F0.4-C1-S2), pattern 7 (F0.6-C1-S2) and Pattern 12 (F1-C1-S2)

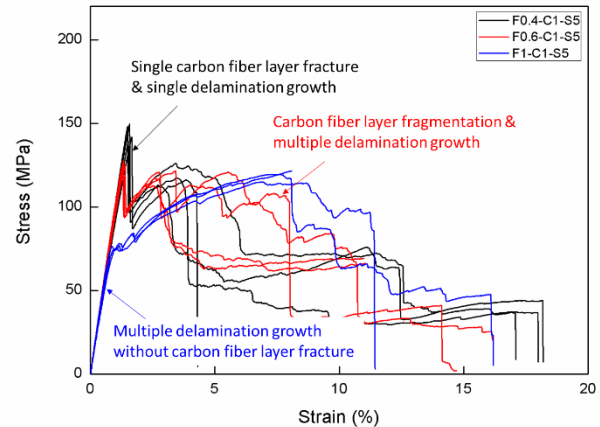


Figure 5: Stress-strain diagrams of pattern 4 (F0.4-C1-S5), pattern 8 (F0.6-C1-S5) and Pattern 13 (F1-C1-S5)

3.2 Effect of the cut length

As illustrated in Table 2, by keeping cut fraction as well as step length the same, seven pairs of two patterns could be compared to reveal the influence of the cut length. When the cut length increases from 0.25 mm to 1 mm, the average number of carbon ply fractures changes in three different ways: (1) staying the same (eg. Pattern 1 vs. pattern 3); (2) increasing (eg. pattern 11 vs. pattern 14); (3) decreasing (eg. pattern 5 vs. pattern 7). Therefore, no consistent tendency has been found to conclude the effect of cut length.

Ideally, decreasing the cut length for a given cut fraction actually creates more fiber bundles. The increase of fiber bundle fracture surface should lead to more energy dissipation, and hence a higher toughness. This hypothesis can be validated from the pure pulling out mechanisms, see Figure 6. The stress-strain curves deviate from the linear region at a low overall strain, which indicates the initiation of fiber bundle pull-out. After that, the black curves (C=0.25 mm, more fiber bundles) show a slight

higher stress level than the red curves ($C=1$ mm, less fiber bundles). The slightly higher increase in stress results in higher toughness (calculated as the area under the curve), until fracture occurs first in the black curves. However, this behavior is not consistent for other cases. Neither could this hypothesis help explain the fracture behavior. The reason accounting for the difference in tensile behaviors resulted from cut length is still unknown.

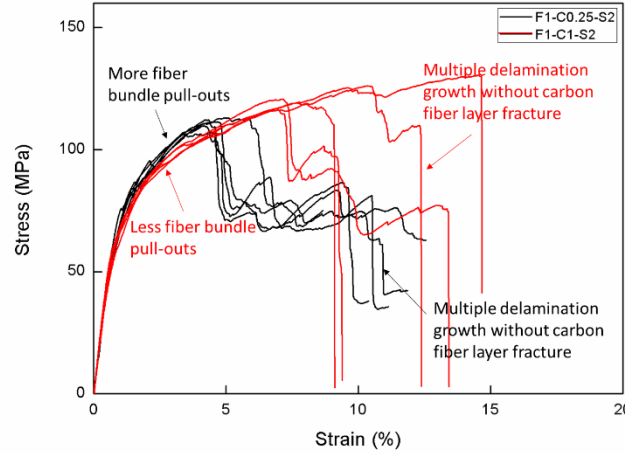


Figure 6: Stress-strain diagrams of pattern 9 (F1-C0.25-S2) and pattern 12 (F1-C1-S2)

3.3 Effect of the step length

According to Table 2, when $F=0.6$ and $C=0.25$ mm, the number of fractures tends to decrease with the increasing of step length. When $F=0.6$ and $C=1$ mm, the same reducing tendency can be found, but the decrease is rather limited (2 compared to 1.75). Figure 7 illustrates the stress-strain curves of patterns that are different in the step length. With the increasing of step length, the peak stress is increased, while multiple fracture transitioned to a single fracture.

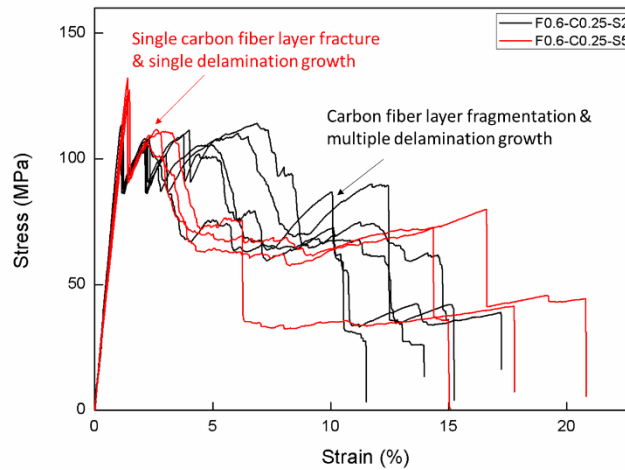


Figure 7: Stress-strain diagrams of pattern 5 (F0.6-C0.25-S2) and pattern 6 (F0.6-C0.25-S5).

As for $F=1$, $C=0.25$ mm (pattern 9 to pattern 11), the average number of fractures first goes up and then down with the increasing of the step length. There is no carbon layer fracture in the case of $S=2$ mm, so the stress strain curves (see black curves in Figure 8) are smooth. The deviation from linear region of the black curves also indicates a low damage resistance. When the step length is increased to 5 mm, several small stress drops appear, which are caused by fiber bundle fracture. When the step length is increased to 10 mm, multiple small stress drops are replaced by one large stress drop, which is also due to carbon fiber bundle fracture. As shown in Figure 9, for layups with $F=1$, $C=1$ mm (pattern 12 to pattern 14), there is no carbon layer fracture when $S=2$ mm and $S=5$ mm, while multiple fractures are achieved when $S=10$ mm.

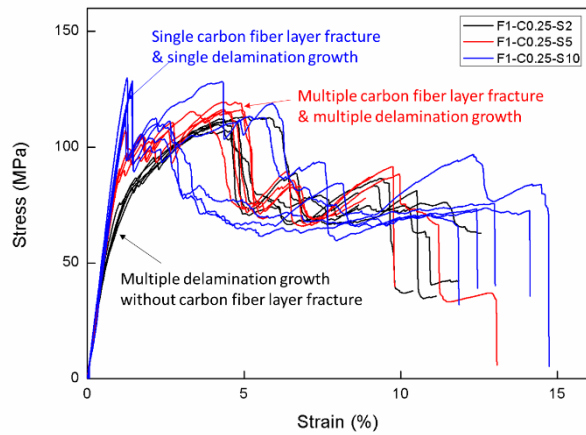


Figure 8: Stress-strain diagrams of pattern 9 (F1-C0.25-S2), pattern 10 (F1-C0.25-S5) and pattern 11 (F1-C0.25-S10)

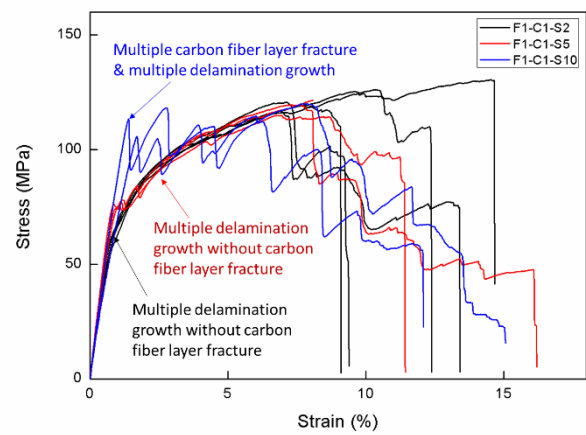


Figure 9: Stress-strain diagrams of pattern 12 (F1-C1-S2), pattern 13 (F1-C1-S5) and pattern 14 (F1-C1-S10)

The peak stress goes up with increased step length, which implies an increasing fracture resistance of the carbon fiber layer. The fiber bundle with longer step length is more likely to fracture than being pulled out. This is reasonable, because the longer the step length is, the easier the stress build-up in the carbon fiber bundle reaches the carbon fiber strength.

3.4 Failure mode map

After analyzing the effect of cut fraction, cut length and step length individually, the isolated effects of the three parameters could not be extracted. The failure mechanisms of the hybrid composites were found to be influenced by all three parameters simultaneously. To reduce the analysis complexity, the step length (S) is divided by the cut length (C), which generates a new combined parameter, called the aspect ratio (W).

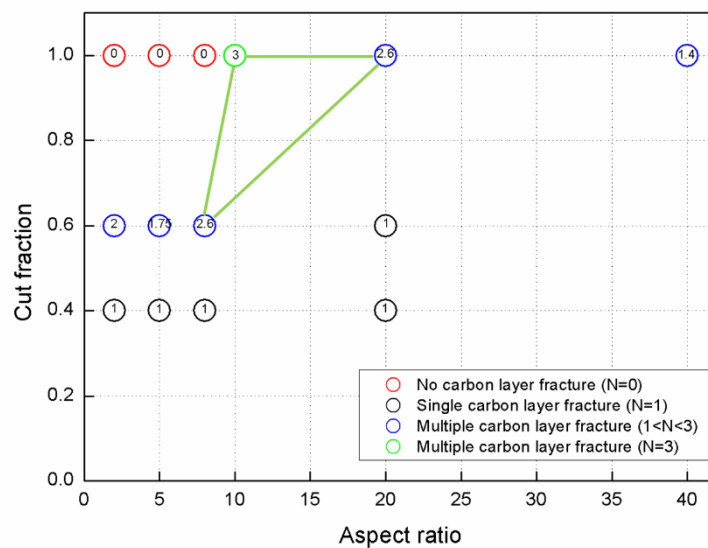


Figure 10: Failure mode map as a function of cut fraction and aspect ratio

Figure 10 shows failure modes for all 14 patterns as a function of the cut fraction and the aspect ratio. The number in the center of the circles indicates the average number of fractures (N). In the case of 0.4 cut fraction, all the patterns show only one fracture. When the cut fraction increases to 0.6, the sample tends to have more carbon fiber layer fractures with the increasing of aspect ratio (but lower than

10), after that, the number of fractures goes down, there might be an upper limit for having multiple fractures in between aspect ratio 10 and 20. For the cut fraction of 1, as the aspect ratio goes up, the failure mechanism changes from no fracture to multiple fractures, then tends to fracture only once at higher aspect ratios. It seems that the region within the green triangle is the region of interest, in which the hybrid composites tend to have more fractures followed by multiple delamination growth, thus creating a gradual failure with relatively high damage resistance. However, this still needs to be confirmed by testing more cutting patterns with different aspect ratios.

4 CONCLUSIONS

Different staggered cutting patterns were introduced in the carbon fiber layer of hybrid carbon fiber/SRPP composites to control the failure mechanisms, hence achieving a gradual failure behavior under tension. The effect of three cutting pattern parameters: cut fraction, cut length and step length were investigated. The following conclusions were drawn:

- The tensile behavior of hybrid carbon fiber/SRPP composites with staggered discontinuities is governed by a combined effect of the cutting pattern parameters. The effect of individual parameters on the tensile behavior could not be isolated.
- When the cut fraction is equal to 0.4, carbon fiber layer fragmentation could not be triggered within the tested range of cut lengths and step lengths.
- Dividing step length by cut length (called aspect ratio) was found to be the more relevant parameter in controlling the tensile behavior for a given cut fraction.
- The gradual failure with relatively high damage resistance is in favour of triggering more carbon layer fractures followed by multiple delamination growth.

ACKNOWLEDGEMENTS

Jun Tang would like to thank China Scholarship Council for supporting his PhD at KU Leuven. Yentl Swolfs acknowledges FWO Flanders for his postdoctoral fellowship. Gianmaria Bullegas and Silvestre Pinho are grateful to the funding from EPSRC under grant EP/M002500/1.

REFERENCES

- [1] S. Bechtle, S. F. Ang, and G. A. Schneider, On the mechanical properties of hierarchically structured biological materials, *Biomaterials*, 31(25), 2010, pp. 6378–6385.
- [2] H. D. Espinosa, J. E. Rim, F. Barthelat, and M. J. Buehler, Merger of structure and material in nacre and bone – Perspectives on de novo biomimetic materials, *Progress in Materials Science*, 54(8), 2009, pp. 1059–1100.
- [3] P. Feraboli, T. Cleveland, M. Ciccu, P. Stickler, and L. DeOto, Defect and damage analysis of advanced discontinuous carbon/epoxy composite materials, *Composites Part A: Applied Science and Manufacturing*, 41(7), 2010, pp. 888–901.
- [4] P. Feraboli, E. Peitso, T. Cleveland, P. B. Stickler, and J. C. Halpin, Notched behavior of prepreg-based discontinuous carbon fiber/epoxy systems, *Composites Part A: Applied Science and Manufacturing*, 40(3), 2009, pp. 289–299.
- [5] I. Taketa, T. Okabe, and A. Kitano, A new compression-molding approach using unidirectionally arrayed chopped strands, *Composites Part A: Applied Science and Manufacturing*, 39(12), 2008, pp. 1884–1890.
- [6] H. Li, W. X. Wang, Y. Takao, and T. Matsubara, New designs of unidirectionally arrayed chopped strands by introducing discontinuous angled slits into prepreg, *Composites Part A: Applied Science and Manufacturing*, 45, 2013, pp. 127–133.
- [7] I. Taketa, T. Okabe, and A. Kitano, Strength improvement in unidirectional arrayed chopped strands with interlaminar toughening, *Composites Part A: Applied Science and Manufacturing*, 40(8), 2009, pp. 1174–1178.
- [8] P. J. Hinea, H. R. Lustib, and A. A. Gusevb, Numerical simulation of the effects of volume fraction, aspect ratio and fibre length distribution on the elastic and thermoelastic properties of short fibre composites, *Composites Science and Technology*, 62, 2002, pp. 1445–1453.

- [9] M. Mirkhalaf, a K. Dastjerdi, and F. Barthelat, Overcoming the brittleness of glass through bio-inspiration and micro-architecture, *Nature Communications*, 5, 2014, pp. 3166.
- [10] G. Bullegas, S. T. Pinho, and S. Pimenta, Engineering the translaminar fracture behaviour of thin-ply composites, *Composites Science and Technology*, 131, 2016, pp. 110–122.
- [11] Y. Swolfs, L. Crauwels, E. Van Breda, L. Gorbatiikh, P. Hine, I. Ward, and I. Verpoest, Tensile behaviour of intralayer hybrid composites of carbon fibre and self-reinforced polypropylene, *Composites Part A: Applied Science and Manufacturing*, 59, 2014, pp. 78–84.
- [12] H. Yu, M. L. Longana, M. Jalalvand, M. R. Wisnom, and K. D. Potter, Pseudo-ductility in intermingled carbon/glass hybrid composites with highly aligned discontinuous fibres, *Composites Part A: Applied Science and Manufacturing*, 73, 2015, pp. 35–44.
- [13] G. Czél, S. Pimenta, M. R. Wisnom, and P. Robinson, Demonstration of pseudo-ductility in high performance glass/epoxy composites by hybridisation with thin-ply carbon prepreg, *Composites Science and Technology*, 106, 2015, pp. 110–119.
- [14] Y. Swolfs, M. Yang, Y. Meerten, J. Ivens, and L. Gorbatiikh, The Effect of Fibre Cuts on the Tensile Behaviour of Hybrid Carbon Fibre / Self-Reinforced Polypropylene, *20th International Conference on Composite Materials*, Copenhagen, July, 2015, pp. 19–24.
- [15] G. Czél, M. Jalalvand, and M. R. Wisnom, Demonstration of pseudo-ductility in unidirectional hybrid composites made of discontinuous carbon/epoxy and continuous glass/epoxy plies, *Composites Part A: Applied Science and Manufacturing*, 72, 2015, pp. 75–84.
- [16] Y. Swolfs, L. Crauwels, L. Gorbatiikh, and I. Verpoest, The influence of weave architecture on the mechanical properties of self-reinforced polypropylene, *Composites Part A: Applied Science and Manufacturing*, 53, 2013, pp. 129–136.